

# Pathomorphological parameters of sepsis-associated encephalopathy in deceased septic patients without purulent lesions to the brain

T. V. Shulyatnikova \*<sup>A,B,C,D</sup>, L. M. Tumanska <sup>A,D,E,F</sup>

Zaporizhzhia State Medical and Pharmaceutical University, Ukraine

A – research concept and design; B – collection and/or assembly of data; C – data analysis and interpretation; D – writing the article; E – critical revision of the article; F – final approval of the article

## Keywords:

sepsis-associated encephalopathy, sepsis-associated liver injury, neuropathology, immunohistochemistry, ammonia, Alzheimer type 2 astrocytes, microglia, amyloid bodies.

## Ключові слова:

сепсис-асоційована енцефалопатія, сепсис-асоційоване пошкодження печінки, патоморфологія, імуногістохімія, аміак, астроцити Альцгеймера 2 типу, амебоїдна мікроглія, амілоїдні тільця.

Надійшла до редакції / Received: 22.04.2024

Після доопрацювання / Revised: 06.05.2024

Схвалено до друку / Accepted: 16.05.2024

**Конфлікт інтересів:** відсутній.

**Conflicts of interest:** authors have no conflict of interest to declare.

## \*E-mail:

shulyatnikova.tv@gmail.com

Sepsis-associated encephalopathy (SAE) clinically manifests by delirium and decreased consciousness less than 15 points on Glasgow Coma Scale. SAE pathophysiology includes neuroinflammation, ischemic-hypoxic and dysmetabolic mechanisms. Despite the high frequency and the important role in thanatogenesis, pathomorphological criteria of SAE remain to be defined.

**The aim** of the study was to specify the key pathomorphological parameters of sepsis-associated encephalopathy in deceased septic patients without purulent lesions to the brain by defining the changes of neurogliovascular unit and the level of tissue ammonia.

**Material and methods.** Using pathohistological, histochemical, and immunohistochemical methods we studied cerebral cortex and white matter, hippocampus, thalamus, and cerebellum of 35 deceased septic patients with SAE in comparison with the control group, which included 30 patients who died from acute cardiovascular failure without CNS pathology.

**Results.** In SAE, small foci of encephalolysis due to thrombosis of microvessels, ischemic-hypoxic and apoptotic changes in neurons are associated with the following parameters that are reliably ( $p < 0.05$ ) different from the control group: higher (up to 199.48 %) level of tissue ammonia and increased number (up to 316.07 %) of caspase-3+ apoptotic neurons in the cortex, hippocampus, thalamus, and cerebellum; in all studied brain regions, an increased expression level of astrocytic glial fibrillary acidic protein (up to 192.69 %), glutamine synthetase (up to 134.41 %) and aquaporin-4 (up to 400.8 %); significant (up to 947.01 %) expansion of perivascular and pericellular "edematous" spaces, increased (up to 479.58 %) immunopositive area of extravascular CD68+ microglia and increased (up to 374.43 %) proportion of CD68+ amoeboid microglia, increased (up to 3.66 times) number of Alzheimer type 2 astrocytes in cerebral cortex, thalamus, and cerebellum; increased (up to 2 times) number of amyloid bodies in the thalamus and cerebellum.

**Conclusions.** The obtained data indicate that the delirious state, loss of consciousness and other manifestations of SAE are associated with ischemic-hypoxic and ammonia-induced ischemic and apoptotic changes of the brain neurons; small foci of encephalolysis; adaptive remodeling and dystrophic changes of astrocytes; microglial reactivity with increased proportion of phagocytic microglia; brain edema and dysfunctional glymphatics.

**Modern medical technology. 2024;16(2):77-85**

## Патоморфологічні параметри сепсис-асоційованої енцефалопатії в померлих хворих на сепсис без гнійного ураження головного мозку

T. V. Shulyatnikova, L. M. Tumanska

Сепсис-асоційовану енцефалопатію (САЕ) клінічно виявляють за депіріозним станом і зниженням свідомості хворих нижче за 15 балів за шкалою ком Глазго. Патологія САЕ включає нейрозапалення, ішемічно-гіпоксичні та метаболічні зміни тканини головного мозку (ГМ). Незважаючи на високу частоту розвитку та важливу роль у танатогенезі, патоморфологічні критерії САЕ залишаються невизначеними.

**Мета роботи** – встановити основні патоморфологічні зміни нейрогліоаскулярного комплексу та рівня тканинного аміаку в головному мозку при сепсис-асоційованій енцефалопатії у померлих хворих на сепсис без гнійного ураження головного мозку.

**Матеріали і методи.** Патогістологічними, гістохімічними, імуногістохімічними методами досліджено кору та білу речовину великих півкуль ГМ (ВПГМ), гіпокамп, таламус і мозочок 35 померлих хворих на сепсис і САЕ. Отримані показники порівняли з параметрами групи контролю, яка включала 30 померлих від гострої серцево-судинної недостатності пацієнтів без патології центральної нервової системи.

**Результати.** При САЕ дрібні осередки енцефалолізу через тромбоз мікросудин, ішемічно-гіпоксичні й апоптотичні зміни нейронів у ГМ асоційовані з такими параметрами контрольної групи, що достовірно відрізнялися ( $p < 0.05$ ): у корі ВПГМ, гіпокампі, таламусі та мозочку визначено вищий рівень (до 199,48 %) тканинного аміаку та більшу кількість (до 316,07 %) каспаза-3+ апоптотичних нейронів; у всіх досліджених

відділах ГМ встановлено підвищений рівень експресії астроцитарного гліофібрилярного білка (до 192,69 %), глутамінсинтетази (до 134,41 %) та аквапорину-4 (до 400,8 %), значне (до 947,01 %) розширення периваскулярних і перичелюлярних «набрякових» просторів, більшу площу (до 479,58 %) експресії позасудинних CD68+ мікрогліоцитів і більшу частку (до 374,43 %) CD68+ амебоїдних мікрогліоцитів; у корі ВПГМ, таламусі та мозочку зафіксовано більшу кількість (до 3,66 раза) астроцитів Альцгеймера 2 типу; у таламусі та мозочку встановлено більшу кількість (до 2 разів) амілоїдних тілець.

**Висновки.** Результати свідчать, що деліріозний стан, зниження свідомості та інші прояви САЕ асоційовані з ішемічно-гіпоксичними й аміак-індукованими ішемічними, апоптотичними змінами нейронів ГМ, дрібними осередками енцефалолізу, адаптивним ремоделюванням і дистрофічними змінами астроцитів, активацією реактивної мікроглії зі збільшенням частки мікрогліоцитів, що фагоцитують, а також набряком ГМ і дисфункцією глімфатичної системи.

**Сучасні медичні технології. 2024. Т. 16, № 2(61). С. 77-85**

According to “Sepsis-3”-2016 consensus, sepsis is defined as a life-threatening organ dysfunction conditioned by dysregulated host response to infection and can develop as sepsis or septic shock [1]. According to the pathomorphological features, both types can manifest in two main forms – septicemia and septicopyemia, although these types of sepsis are not separately defined in ICD-10. During septicopyemia, sepsis-induced brain damage morphologically manifests by a metastatic septic-embolic brain abscesses, meningoencephalitis, purulent ventriculitis, vasculitis, as well as multiple microhemorrhages, microvascular thrombosis and microinfarcts mainly in the cerebral white matter [2].

Sepsis-associated encephalopathy (SAE) is widely considered as infectious non-invasive damage to the brain, which is clinically manifested by delirium and decreased patients' consciousness below 15 points on the Glasgow coma scale (GCS) in the exclusion of other potential neuroaggressive factors [3]. SAE can develop both in septicemia and in septicopyemia without purulent lesions to the brain. Simultaneously, B. H. Singer et al. using the cultural PCR-gene sequencing of brain tissue provided evidence for the presence of viable intestinal type bacteria in the rodent brain in CLP-abdominal sepsis and in the postmortem brain of septic patients without metastatic abscess [4]. The latter causes some uncertainty of the pathogenetic factors of SAE initiation. The pathophysiology of SAE includes neuroinflammation, ischemic damage, and metabolic shifts in neural tissue. Recently, hyperammonemia was proven as important factor of neuroaggression in sepsis. It can cause the so-called hyperammonemic encephalopathy and can be conditioned by multiple organ dysfunction syndrome (MODS), specific infection, the side effect of certain pharmaceuticals, and other factors [5,6].

A common component of septic MODS, which most likely causes hyperammonemia, is sepsis-associated liver injury (SALI), which clinically manifests as cholestasis, hypoxic hepatitis, and coagulopathy and is accompanied by a decrease in the synthetic, detoxification, and excretory liver functions [7]. Recently, hyperammonemia has been proposed as a new biomarker of sepsis and independent risk factor for short-term mortality of septic patients [8,9] including SAE patients without liver injury [6]. Brain pathomorphological changes in deceased septic patients with SALI and experimental CLP-rats were partially described in our previous studies [10] and included increased histochemical (HC) tissue ammonia levels, appearance of Alzheimer type 2 astrocytes (AA2), and increased expression of astroglial proteins GFAP, GS, and AQP4.

In addition to the uncovered pathomorphological changes in other components of the neurogliovascular unit (NGVU), the question remains whether such changes are present and how pronounced they are in the brain of deceased septic patients with intravitaly confirmed SAE, and whether they can be used for postmortem diagnosis of SAE.

## Aim

The aim of the study was to specify the key pathomorphological parameters of sepsis-associated encephalopathy in deceased septic patients without purulent lesions to the brain by defining the changes of neurogliovascular unit and the level of tissue ammonia.

## Materials and methods

The study was performed on autopsy material of 35 deceased patients with abdominal sepsis (mean age  $67.65 \pm 6.36$  y. o.), who had a decrease in consciousness less than 15 points of GCS (SAE) 1–12 days before death; median values of GCS were 9.00 (6.00; 12.00) points. Cases of septic meningoencephalitis, including abscess encephalitis, as well as chronic liver disease, alcoholism, endocrine diseases, and other chronic toxic-metabolic diseases were excluded from the study. The causative factors of abdominal sepsis were represented by complications of peptic ulcer disease of stomach and duodenum, as well as inflammatory bowel diseases ( $n = 21$ ; 60.00 %), and pancreonecrosis ( $n = 14$ ; 40.00 %). 20 (57.14 %) of the 35 patients were diagnosed with signs of SALI accompanied by liver dysfunction / failure, which was characterized by an increase in serum bilirubin (according to Sequential Organ Failure Assessment score, SOFA) and was morphologically confirmed by the presence of focal lymphohistiocytic infiltration of the portal tracts, fatty dystrophy and small foci centrilobular necrosis of hepatocytes, focal proliferation of ductular epithelium, dilation of bile capillaries with cholestasis. Among other components of MODS according to the SOFA scale, signs of other forms of organ dysfunction / failure were observed in patients during their lifetime: renal ( $n = 22$ ; 62.85 %) and cardiovascular ( $n = 29$ ; 82.85 %) (according to the level of serum creatinine and mean arterial pressure respectively), coagulopathy ( $n = 16$ ; 45.71 %) (according to the level of thrombocytopenia), and in 26 cases (74.28 %) signs of respiratory failure against the background of focal purulent-fibrinous pneumonia and/or respiratory distress syndrome of adults were determined (Table 1).

**Table 1.** Distribution of organ dysfunction / failure in deceased sepsis patients with CAE

Patient's No. in order	Organ dysfunction / failure					
	SAE (points)	Liver	Kidney	Circulatory	Lungs	Coagulopathy
1	GCS = 10	–	–	+	+	–
2	GCS = 12	–	+	+	–	+
3	GCS = 9	+	–	+	+	+
4	GCS = 8	+	+	+	+	–
5	GCS = 12	–	+	+	–	–
6	GCS = 13	–	–	+	–	–
7	GCS = 6	+	+	–	+	+
8	GCS = 7	+	–	+	+	–
9	GCS = 11	–	+	–	+	–
10	GCS = 12	–	+	+	–	+
11	GCS = 6	+	+	+	+	–
12	GCS = 6	+	+	+	+	–
13	GCS = 5	+	+	+	+	+
14	GCS = 13	–	+	+	–	–
15	GCS = 6	+	+	+	+	+
16	GCS = 7	+	+	+	+	+
17	GCS = 5	+	+	+	+	–
18	GCS = 9	+	–	+	+	–
19	GCS = 6	+	+	+	+	+
20	GCS = 13	–	–	+	–	–
21	GCS = 9	+	–	–	+	+
22	GCS = 6	+	+	+	+	+
23	GCS = 12	–	–	+	–	+
24	GCS = 10	–	+	+	+	–
25	GCS = 12	–	–	+	–	–
26	GCS = 6	+	+	+	+	+
27	GCS = 5	+	+	+	+	+
28	GCS = 7	+	+	+	+	–
29	GCS = 10	+	–	–	+	–
30	GCS = 12	–	–	+	–	–
31	GCS = 6	+	+	+	+	+
32	GCS = 5	+	+	+	+	+
33	GCS = 11	–	–	–	+	–
34	GCS = 10	–	+	–	+	–
35	GCS = 9	–	–	+	+	+

**GCS:** Glasgow Coma Scale; +: presence; –: absence.

The conditional control group included patients who died from acute cardiovascular failure, without toxic-metabolic pathology and brain diseases (n = 30).

Sectional material was collected in the amount recommended for routine pathological diagnosis of the diseases. Cortical samples from the frontal, parietal, temporal, and occipital lobes of the cerebral large hemispheres, thalamus, striatum, and cerebellum were fixed in 10 % buffered formalin and embedded in paraffin blocks. Serial 4 µm sections for microscopic analysis (hematoxylin and eosin staining), histochemical (HC) and immunohistochemical (IHC) studies were produced by the precession rotary microtome HM3600 ("MICROM Laborgerate GmbH", Germany). Ammonia determination in paraffin brain sections was performed by HC method using Nessler's reagent according to V. Gutiérrez-de-Juan et al. [11]. IHC studies were performed in paraffin sections using the UltraVision Quanto HRP + DAB System visualization system (Thermo Scientific, USA). The level of neuronal apoptotic changes was detected using Mo a-Hu Caspase 3 (Casp3) (CPP32) Ab-3 (Clone 3CSP03, Thermo Scientific Inc., USA); synaptic vesicles quantities in presynaptic terminals were identified by Mo anti-synaptophysin (Syn) Ab (Clone SY38, Thermo Scientific Inc., USA); to identify astrocytic changes were used Mo anti-GFAP Ab (Clone ASTRO6, Thermo Scientific Inc., USA), Rb polyclonal anti-GS Ab (Thermo Scientific Inc., USA) and Rb polyclonal anti-AQP4 Ab (Thermo Scientific Inc., USA); microglia and ameboid microgliaocytes were identified by Mo a-Hu CD68 Ab (clone PG-M1, Dako, Denmark).

Morphometric analysis was performed in the microscope Scope A1 "Carl Zeiss" (Germany) with camera Jenoptik Progres Gryphax 60N-C1"1,0x426114 (Germany) using morphometric software. HC ammonia expression and IHC expression of synaptophysin were determined in ImageJ (National Institutes of Health, USA) using automatic mode with standard plug-in colour deconvolution "H DAB" in 5 standardized fields of view (SFV) ×200 of four mentioned brain regions in each case and were expressed in conventional units of optical density (CUOD). With CUOD values from 0 to 20, ammonia and synaptophysin expression were considered negative ("−"); 21–50 – weak ("+"); 51–100 – moderate ("++"); ≥101 – strong ("+++").

Using Videotest-Morphology 5.2.0.158 (LLC "VideoTest") software, in 5 SFV ×200 of each case, in four brain regions were determined the relative area (Srel. %) of immunopositive material of GFAP, GS, AQP4, and CD68, the percentage of Caspase 3+ neurons (%), and at magnification ×400 – percentage of CD68+ ameboid microgliaocytes (%). In each studied brain region, in 5 SFV ×400, the mean area of "empty" (swollen) pericellular and perivascular spaces (µm<sup>2</sup>) as well as the average number of amyloid bodies (AB) were calculated. In 20 SFV of each case, the number of Alzheimer type 2 astrocytes was determined and 4 degrees of AA2-astrocytosis were identified: 1–5 AA2 – 0 degree; 6–10 AA2 – I degree (weak AA2-astrocytosis); 11–20 AA2 – II degree (moderate); 21 or more AA2 – III degree (severe) [10].

Data were processed using the Statistica ®13.0 package (StatSoft Inc., License No. JPZ804I382130ARCN10-J). Results were represented as median (Me) with range (Q1; Q3). The Mann–Whitney U-test was used to compare two groups, and

the Kruskal–Wallis test was used for two or more groups. The results were considered statistically significant at the level of 95 % (p < 0.05).

## Results

Regardless of the causative factor of abdominal sepsis, as well as its clinical (sepsis / septic shock) and pathomorphological (septicaemia / septicopyemia) course, pathohistological examination revealed diffuse focal microvascular thrombosis, small foci of encephalolysis, microhemorrhages mainly in the cerebral cortex, white matter and hippocampus. In all cases, hemomicrocirculatory disorders were combined with apoptotic and ischemic changes in neurons, widespread and variably expressed perineuronal glial satellitosis and predominantly perivascular edema. The comprehensive study showed that the parameters of the brain NGVU in deceased patients with SAE significantly and reliably differ from the control indicators.

In SAE patients, four out of five studied brain regions were characterized by weak to moderate granular expression of ammonia precipitates, which reliably (p < 0.05) exceeded the indicators of the control group with negative ammonia expression. In the cortex this relation was 34.31 (25.73; 62.12) vs 18.14 (15.26; 19.53) CUOD (89.14 % higher); hippocampus – 25.26 (21.73; 34.56) vs 17.25 (14.68; 18.72) CUOD (46.43 % higher); thalamus – 57.65 (53.41; 87.16) vs 19.25 (16.58; 19.72) CUOD (199.48 % higher); cerebellum – 50.67 (47.42; 81.14) vs 19.74 (18.32; 19.83) CUOD (156.68 % higher), respectively (Fig. 1, 2). By this, cortical and hippocampal ammonia expression defined as weak ("+"), while thalamic and cerebellar as moderate ("++"). Cerebral white matter showed only a tendency to increase ammonia expression, which was not statistically significant (p > 0.05).

An increase in brain tissue ammonia in SAE was associated with structural and functional remodeling of NGVU cells. Hematoxylin-eosin stained sections of the cortex, hippocampus, thalamus, and cerebellum showed mainly ischemic-changed and apoptotic neurons that had reduced, compact, triangular profiles.

Simultaneously, IHC revealed significantly (p < 0.05) higher percentage of Caspase-3+ apoptotic neurons compared to control: in the cortex, the relation was 17.35 (12.16; 18.12) % vs 5.63 (3.29; 8.68) % (208.17 % higher); hippocampus – 15.27 (14.86; 16.56) % vs 3.67 (2.83; 5.36) % (316.07 % higher); thalamus – to 12.15 (10.83; 17.82) % vs 3.25 (2.74; 4.67) % (273.84 % higher); cerebellum – 12.57 (11.43; 16.14) % vs 4.25 (2.16; 5.24) % (195.76 % higher), respectively (Fig. 1, 3). In addition to signs of neuronal death, the minor tendency (p > 0.05) to decrease in the neuronal synaptic transmission was found by the reduced optical density of Synaptophysin: in the cortex – 54.52 (50.86; 67.38) CUOD vs 61.65 (56.23; 71.34) CUOD; hippocampus – 51.24 (49.72; 65.95) CUOD vs 54.72 (51.12; 58.63) CUOD; thalamus – 53.61 (51.73; 64.48) CUOD vs 60.48 (57.92; 65.35) CUOD; cerebellum – 49.45 (45.68; 50.21) CUOD vs 51.37 (48.63; 53.92) CUOD, respectively (Fig. 1).

In SAE brain significant reactive changes were observed in astrocytes. Thus, GFAP, the main astrocytic cytoskeletal protein, showed a significant and reliable (p < 0.05) growth compared to control in all studied brain regions: in the cortex – 13.23 (12.67;

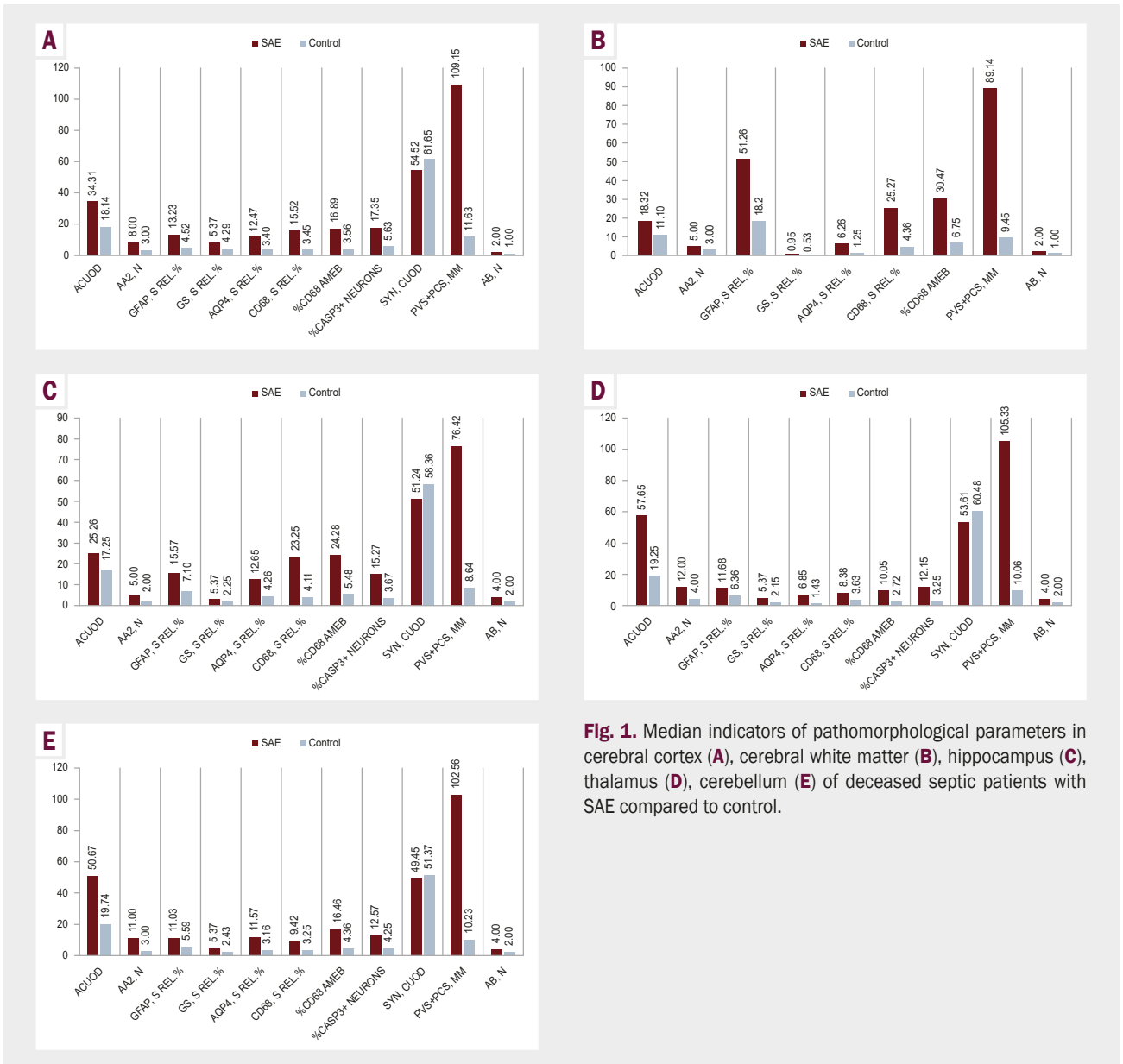


**Fig. 1.** Median indicators of pathomorphological parameters in cerebral cortex (A), cerebral white matter (B), hippocampus (C), thalamus (D), cerebellum (E) of deceased septic patients with SAE compared to control.

22.65) % vs 4.52 (4.23; 5.57) % (192.69 % higher); white matter – 51.26 (46.85; 53.41) % vs 18.20 (17.11; 18.43) % (181.64 % higher); hippocampus – 15.57 (14.69; 18.14) % vs 7.10 (6.58; 7.89) % (119.29 % higher); thalamus – 11.68 (8.59; 12.42) % vs 6.36 (5.91; 6.79) % (83.64 % higher); cerebellum – 11.03 (9.52; 14.47) % vs 5.59 (5.18; 5.83) % (97.31 % higher), respectively (Figs. 1, 4).

At the same time, reliable ( $p < 0.05$ ) increase in the level of the astrocyte-specific ammonia detoxification enzyme GS was determined in the cortex – 8.20 (7.11; 12.53) % vs 4.29 (2.26; 5.63) % (91.14 % higher); white matter – 0.95 (0.66; 1.78) % vs 0.53 (0.34; 0.60) % (79.24 % higher); thalamus – 5.04 (4.83; 7.69) % vs 2.15 (1.73; 3.45) % (134.41 % higher); cerebellum – 4.66 (3.11; 6.72) % vs 2.43 (0.63; 2.84) % (91.76 % higher), respectively (Figs. 1, 5). In the hippocampus, GS expression was characterized only by a tendency ( $p > 0.05$ ) to increase compared to control cases – 3.15 (3.02; 5.23) % vs 2.25 (0.53; 3.90) %.

The expression of AQP4, the main water channel protein in the CNS, in SAE brain was also characterized by reliable ( $p < 0.05$ ) elevation comparing to control indicators: in the cortex – 12.47 (11.61; 15.48) % vs 3.40 (3.22; 4.25) % (266.76 % higher); white matter – 6.26 (5.73; 9.84) % vs 1.25 (0.75; 1.34) % (400.8 % higher); hippocampus – 12.65 (11.48; 14.36) % vs 4.26 (4.17; 5.25) % (196.94 % higher); thalamus – 6.85 (6.12; 7.09) % vs 1.43 (0.43; 1.68) % (379.02 % higher); cerebellum – 11.57 (10.05; 13.71) % vs 3.16 (2.47; 3.75) % (266.13 % higher), respectively (Figs. 1, 6). With this, all studied brain regions showed reliably ( $p < 0.05$ ) increased the average area of perivascular and pericellular tissue “edematous” spaces. The medians of the relative area of these spaces were compared as: in the cortex – 109.15 (106.45; 110.46)  $\mu\text{m}^2$  vs 11.63 (9.48; 14.25)  $\mu\text{m}^2$  (838.52 % higher); white matter – 89.14 (84.58; 95.45)  $\mu\text{m}^2$  vs 9.45 (7.24; 9.56)  $\mu\text{m}^2$  (843.28 % higher); hippocampus – 76.42 (73.51; 84.48)  $\mu\text{m}^2$  vs 8.64 (6.38; 9.59)  $\mu\text{m}^2$  (784.49 %

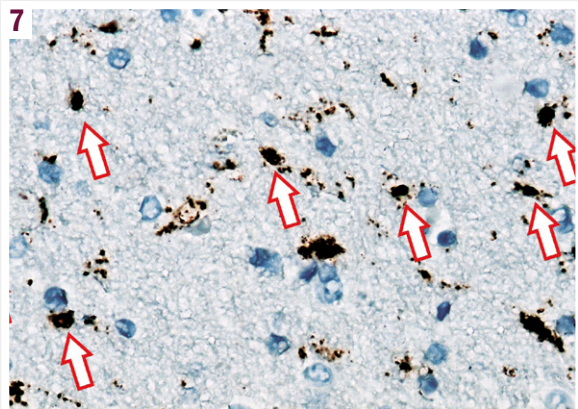
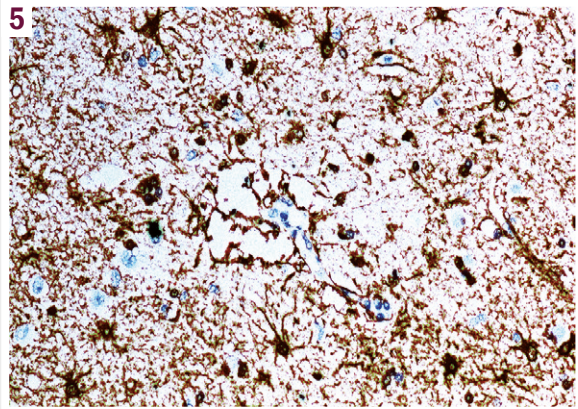
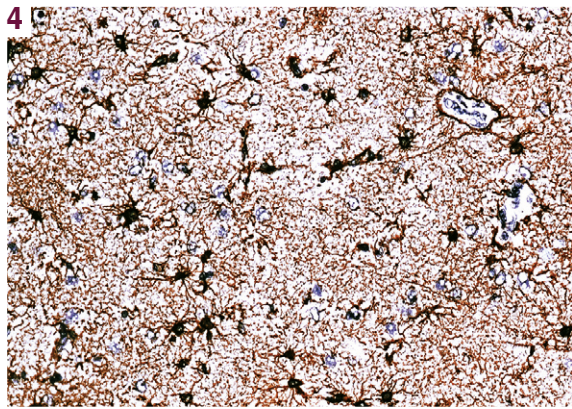
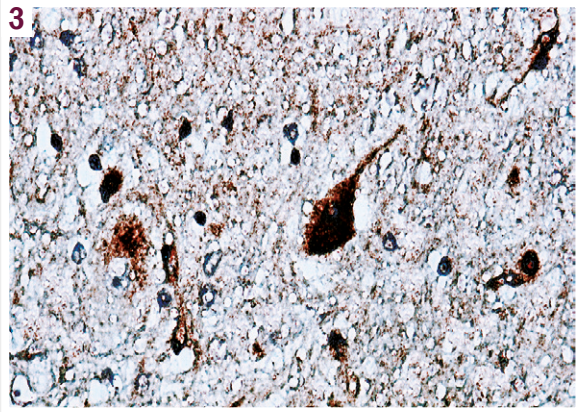
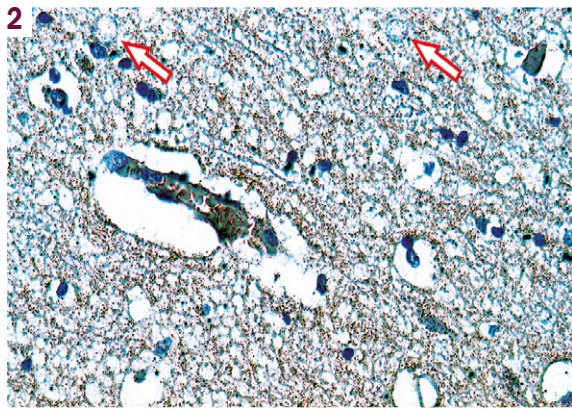


**Fig. 2.** Moderate (“++”) HC ammonia expression (in CUOD) with the presence of single AA2-astrocytes (red arrows) in the thalamus of a deceased septic patient with SAE. HC reaction with Nessler’s reagent. Mg.  $\times 400$ .

**Fig. 3.** Caspase+ neurons in the cortex of a deceased septic patient with SAE. Mo monoclonal antibody – Caspase 3 (CPP32) Ab-3 (clone 3CSP03, Thermo Scientific Inc., USA). Mg.  $\times 400$ .

**Fig. 4.** Hyperexpression of GFAP in the cerebral cortex of a deceased septic patient with SAE. Mo monoclonal anti-GFAP Ab (clone ASTRO6, Thermo Scientific Inc., USA). Mg.  $\times 200$ .

**Fig. 5.** Hyperexpression of GS in the thalamus of a deceased septic patient with SAE. Rb polyclonal anti-GS Ab (Thermo Scientific Inc., USA). Mg.  $\times 400$ .

**Fig. 6.** Hyperexpression of AQP4 in the thalamus of a deceased septic patient with SAE. Rb polyclonal anti-AQP4 Ab (Thermo Scientific Inc., USA). Mg.  $\times 400$ .

**Fig. 7.** Hyperexpression of CD68+ and numerous amoeboid microgliaocytes (red arrows) in the cortex of a deceased septic patient with SAE. Mo a-Hu CD68 Ab (clone PG-M1, RTU, Dako, Denmark) Mg.  $\times 400$ .

higher); thalamus – 105.33 (96.71; 108.44)  $\mu\text{m}^2$  vs 10.06 (8.15; 11.45)  $\mu\text{m}^2$  (947.01 % higher); cerebellum – 102.56 (99.64; 114.06) vs 10.23 (9.98; 11.56)  $\mu\text{m}^2$  (902.54 % higher), respectively (Fig. 1).

A peculiar sign of reactive astrocytic remodeling in the brain is the accumulation of Alzheimer type 2 astrocytes (AA2-astrocytosis). In contrast to control group, where AA2-astrocytosis was absent, the weak (“+” – in the cortex) and moderate (“++” – in the thalamus and cerebellum) AA2-astrocytosis was revealed in the brain of SAE patients. regions of SAE patients. The comparison between the medians of the AA2 number in SAE and control patients was as follows: in the cortex – 8.00 (5.00; 12.00) units vs 3.00 (2.00; 4.00) units (exceeds 2.66 times); thalamus – 12.00 (9.00; 15.50) units vs 4.00 (3.00; 6.00) units (exceeds 3 times); cerebellum – 11.00 (9.00; 11.50) units vs 3.00 (4.00; 6.00) units (exceeds 3.66 times) respectively,  $p < 0.05$  (Figs. 1, 2). In the white matter and hippocampus, despite a statistically significant increase in the AA2 number, AA2-astrocytosis was not determined according to the scale we used.

Brain tissue damage and decay processes, as well as astrocytic dysfunction in SAE brain were proved by the significantly ( $p < 0.05$ ) increased number of amyloid bodies in thalamus and cerebellum (increase up to 2 times): 4.00 (4.00; 5.00) units vs 2.00 (1.00; 3.00) units and 4.00 (3.00; 5.50) units vs 2.00 (1.50; 2.00) units, respectively. In the cortex, white matter, and hippocampus, the number of amyloid bodies did not statistically differ from the control group ( $p > 0.05$ ) (Fig. 1).

The expression area of the extravascular reactive CD68+ microglia was reliably ( $p < 0.05$ ) increased compared to control: in the cortex – 15.52 (11.43; 16.68) % vs 3.45 (2.37; 4.68) % (349.85 % higher); white matter – 25.27 (19.66; 28.59) % vs 4.36 (2.54; 5.12) % (479.58 % higher); hippocampus – 23.25 (8.47; 17.58) % vs 4.11 (2.65; 4.86) % (465.69 % higher); thalamus – 8.38 (7.96; 9.39) % vs 3.63 (2.12; 3.97) % (130.85 % higher); cerebellum – 9.42 (8.93; 10.51) % vs 3.25 (2.44; 4.34) % (189.84 % higher), respectively (Figs. 1, 7).

At the same time, the percentage of CD68+ amoeboid microglia was also significantly ( $p < 0.05$ ) higher compared to control: in the cortex – 16.89 (10.25; 19.32) % vs 3.56 (3.14; 4.26) % (374.43 % higher); white matter – 30.47 (18.86; 33.56) % vs 6.75 (4.48; 8.37) % (351.40 % higher); hippocampus – 24.28 (20.45; 24.49) % vs 5.48 (4.73; 7.29) % (343.06 % higher); thalamus – 10.05 (9.83; 11.46) % vs 2.72 (2.54; 3.69) % (269.48 % higher); cerebellum – 16.46 (15.35; 20.56) % vs 4.36 (3.64; 4.83) % (277.52 % higher), respectively (Figs. 1, 7).

## Discussion

The results of the study showed that the SAE brain is characterized by a significant morpho-functional changes in the NGVU, which can represent the anatomical substrate of the delirious symptoms, as well as loss of patient's consciousness. In a recent study, X. Lu et al. [3] attempted to classify SAE and identified four clinic-pathophysiological phenotypes:

1. ischemic-hypoxic (in hypoxemia and septic shock);
2. metabolic (serum urea nitrogen  $> 17.85$  mmol/l, or glucose  $< 2.5$  mmol/l, or INR  $> 2.5$  and AST or ALT  $> 200$  U/l, or sodium  $< 120/ > 160$  mmol/l);

3. mixed (ischemic-hypoxic + metabolic);
4. unclassified.

The authors point out that the mixed SAE phenotype is associated with the highest risk of in-hospital mortality. Considering the organ failure spectrum in our cohort patients, we can assume that there was no pure metabolic variant of SAE, and only ischemic-hypoxic and mixed types were observed with a significant predominance of the latter. This indicates that in the conditions of severe sepsis with SAE and lethal outcome, the combinative mechanisms of CNS neuroaggression play a golden role. The pathomorphological evidence of the metabolic component of SAE was represented by weak and moderate accumulation of ammonia in thalamus, cerebellum, cortex and, to a lesser extent, in the hippocampus. Considering that, 57.14 % patients were diagnosed with clinical and pathomorphological signs of sepsis-associated liver injury, the accumulation of brain tissue ammonia was most likely caused by liver failure that developed under these conditions.

In addition, recent studies have shown that in critically ill patients of intensive care units (ICU), including those with sepsis, hyperammonemia can be associated with states unrelated to liver damage – “non-hepatic hyperammonemia” (NHHA) [12], which can be caused by increased production, congenital and acquired reduction of ammonia metabolism and excretion [13]. Increased production of ammonia during sepsis can be due to nutritional and enteral reasons, gastrointestinal bleeding, malignant tumors with a high catabolic status, urease-producing infections of the urinary tract and extraurinary localization, chemotherapy. While reduced excretion of ammonia may be due to acute or chronic renal failure, unrecognized congenital or acquired defects of the urea cycle, treatment with anesthetics, analgetics and other pharmaceuticals [12]. These conditions can cause fatal hyperammonemia, but due to their relative rarity, the incidence of diagnosed NHHA in ICU remains low. On the other hand, the latter may be due to the lack of plasma ammonia monitoring in critically ill patients without signs of liver injury [12].

The most likely reasons of NHHA in patients of our study could be renal dysfunction / failure (according to the SOFA scale) (occurred in 62.85 % of patients), gastrointestinal bleeding (occurred in 31.42 % of patients) and parenteral nutrition (in all patients). The ischemic-hypoxic mechanism of NGVU changes occurred in almost all SAE patients, considering that 82.85 % of them had manifestations of cardiovascular failure combined with respiratory failure (in 74.28 % of observations). The ischemic component of NGVU damage in SAE was confirmed by small foci of encephalolysis, ischemic neurons, and increased percentage of apoptotic caspase-3+ neurons in the cortex, hippocampus, thalamus, and cerebellum. Among studied neuron-rich brain regions, the tendency to the greatest increase in the percentage of apoptotic neurons showed hippocampus, as being one of the most hypoxia-sensitive brain structures. Meanwhile, the optical density of synaptic vesicles Synaptophysin protein expression in the interneuronal synapses of the studied regions had only a tendency to decrease, which may indicate less significant contribution of synaptic malfunctions in the development of psychoneurological deficit in SAE patients.

The metabolic component of SAE in the form of tissue ammonia accumulation was associated with the corresponding changes in neuroglia, which were previously partially described by us in septic patients with SALI. Thus, increased level of ammonia-detoxifying astrocytic GS was observed in all studied brain regions with a tendency to maximal values in the thalamus, cerebellum, and cortex, and accompanied by the development of mild-to-moderate Alzheimer-2 astrocytosis in these regions. This combination evidences the active involvement of local astroglial populations in the neutralization of excessive tissue ammonia accompanied by selective astrocytic dysmetabolic dystrophy in the final stages [14,15].

In parallel, the increased expression of the main astrocytic cytoskeletal protein GFAP in all the above-mentioned regions was associated with a tendency to the least pronounced elevation in thalamus and cerebellum, while the maximal – in the white matter, cortex, and hippocampus. Neuroinflammatory mechanisms, which are central in SAE pathogenesis and determine the cascade of vasculo-glio-neuronal stimulation, mutual potentiation and damage, are characterized by reactive remodeling of neuroglia, where the hyperexpression of GFAP is a clear manifestation of reactive astrocytosis. Moreover, the latter can also be caused by ischemic-hypoxic damage to nervous tissue [16] with the development of small foci reactive gliofibrosis.

The greatest increase in GFAP expression in the white matter, cortex, and hippocampus in SAE confirms neuroanatomical observations of other authors considering relatively more significant damage to these brain regions in sepsis [17]. On the other hand, the smallest increase in GFAP expression in the thalamic and cerebellar areas can be explained by the reduced synthesis of these structural proteins under the inhibitory effect of higher concentrations of tissue ammonia [18] in these regions. Interestingly, despite the substantial increase in cortical ammonia, the level of cortical GFAP was also significantly increased. It can be assumed that this is due to a more pronounced neuroinflammatory process and ischemic-hypoxic changes in the cortex, which requires greater intensity and duration of adaptive-reactive astrogliosis. The combined elevation of astrocytic AQP4 expression with the area of “edematous” tissue spaces in all five investigated brain regions during SAE indicates edematous tissue changes that can have both vasogenic and cytotoxic mechanisms and be associated with both ischemia-induced and ammonia-induced overexpression AQP4, as well as glutamine-induced hyperosmolar swelling of the perivascular and neuropil astroglia [19]. Interestingly, the tendency for the highest increase in AQP4 was observed in the white matter and thalamus. If the latter can be explained by the higher tissue ammonia, then the former, most likely, can be associated with more pronounced hypoxic-ischemic mechanisms of aquaporin induction [20].

At the same time, the expansion of the “edematous” tissue spaces was approximately equally expressed among the studied regions with the maximum rates in the thalamus and cerebellum and the lowest values in the hippocampus. The absence of a clear topical correlation between the maximal AQP4 levels and the severity of tissue edema in the white matter can be explained by the low local level of tissue ammonia, which excludes the glutamin-osmotic mechanism and leaves only the ischemic-hypoxic induction of astrocytic edema in this region.

The slight accumulation of amyloid bodies in the thalamus and cerebellum of SAE brain indicates the development of relative astrocytic insufficiency and dysfunction of the glymphatic system of these regions with accumulation of astrocytogenic waste products of tissue metabolism and decay that do not drain into the subarachnoid spaces [21]. The selectivity of amyloid bodies accumulation in these areas may be conditioned by the maximal levels of tissue ammonia observed there.

The trend towards the greatest increase in extravascular microglial CD68 expression, as well as the maximum percentage of phagocytic CD68+ amoeboid microglia in the cortex, white matter, and hippocampus of the SAE brain supposes greater reactivity of the local microglial populations and phagocytosis activation in them. The latter may be caused by with more pronounced ischemic-hypoxic and neuroinflammatory damage to the listed regions, as well as with higher ammonia concentrations in thalamus and cerebellum which can have the inhibitory effect on the phagocytic properties of activated microglia, as shown by I. Zemtsova et al. [22].

## Conclusions

1. In the cerebral cortex and white matter, hippocampus, thalamus, and cerebellum of deceased septic patients with sepsis-associated encephalopathy (compared to control patients who died of acute cardiovascular failure), small foci of encephalolysis due to microvascular thrombosis, ischemic-hypoxic and apoptotic changes in neurons, complex remodeling of astroglia, activation of reactive and phagocytic microglia, as well as tissue edema were determined.

2. The specified brain regions during sepsis-associated encephalopathy are characterized by the following: weak-to-moderate histochemical ammonia expression; significant expansion of the swollen pericellular and perivascular spaces; slight accumulation of amyloid bodies; increased percentage of apoptotic caspase-3+ neurons; increased expression of glutamine synthetase, aquaporin-4 and gliofibrillary acidic protein in astrocytes; weak-to-moderate AA2-astrocytosis; significant increase in microglial CD68 expression with an increased percentage of CD68+ amoeboid microglia.

**Prospects for further research.** Further studies are needed to compare pathomorphological parameters of sepsis-associated and other somatogenic toxic-metabolic encephalopathies to define common and differential features and eventually create the basis for a broader differential diagnosis of various causes of brain dysfunction in critically ill patients.

## Funding

This study was conducted in the framework of the scientific research work of Zaporizhzhia State Medical University “Morphogenesis of destructive-reparative processes of the brain in diseases of vascular and toxic-metabolic genesis”, state registration No. 0118U004253 (2018–2022).

## Information about the authors:

Shulyatnikova T. V., MD, PhD, Associate Professor of the Department of Pathological Anatomy and Forensic Medicine, Zaporizhzhia State Medical and Pharmaceutical University, Ukraine.  
ORCID ID: 0000-0002-0196-9935

Tumanska L. M., MD, PhD, Associate Professor of the Department of Pathological Anatomy and Forensic Medicine, Zaporizhzhia State Medical and Pharmaceutical University, Ukraine.  
ORCID ID: 0000-0001-5715-0040

#### Відомості про авторів:

Шулятникова Т. В., канд. мед. наук, доцент каф. патологічної анатомії і судової медицини, Запорізький державний медико-фармацевтичний університет, Україна.

Туманська Л. М., канд. мед. наук, доцент каф. патологічної анатомії і судової медицини, Запорізький державний медико-фармацевтичний університет, Україна.

#### References

- Guarino M, Perna B, Cesaro AE, Maritati M, Spampinato MD, Contini C, et al. 2023 Update on Sepsis and Septic Shock in Adult Patients: Management in the Emergency Department. *J Clin Med*. 2023;12(9):3188. doi: [10.3390/jcm12093188](https://doi.org/10.3390/jcm12093188)
- Garofalo AM, Lorente-Ros M, Goncalvez G, Carriedo D, Ballén-Barragán A, Villar-Fernández A, et al. Histopathological changes of organ dysfunction in sepsis. *Intensive Care Med Exp*. 2019;7(Suppl 1):45. doi: [10.1186/s40635-019-0236-3](https://doi.org/10.1186/s40635-019-0236-3)
- Lu X, Qin M, Walline JH, Gao Y, Yu S, Ge Z, et al. Clinical phenotypes of sepsis-associated encephalopathy: a retrospective cohort study. *Shock*. 2023;59(4):583-90. doi: [10.1097/SHK.0000000000002092](https://doi.org/10.1097/SHK.0000000000002092)
- Singer BH, Dickson RP, Denstaedt SJ, Newstead MW, Kim K, Falkowski NR, et al. Bacterial Dissemination to the Brain in Sepsis. *Am J Respir Crit Care Med*. 2018;197(6):747-756. doi: [10.1164/rccm.201708-1559OC](https://doi.org/10.1164/rccm.201708-1559OC)
- Zhao L, Walline JH, Gao Y, Lu X, Yu S, Ge Z, et al. Prognostic Role of Ammonia in Critical Care Patients Without Known Hepatic Disease. *Front Med (Lausanne)*. 2020;7:589825. doi: [10.3389/fmed.2020.589825](https://doi.org/10.3389/fmed.2020.589825)
- Zhao L, Hou S, Na R, Liu B, Wang Z, Li Y, Xie K. Prognostic role of serum ammonia in patients with sepsis-associated encephalopathy without hepatic failure. *Front Public Health*. 2023;10:1016931. doi: [10.3389/fpubh.2022.1016931](https://doi.org/10.3389/fpubh.2022.1016931)
- Woźnica EA, Ingłot M, Woźnica RK, Łysenko L. Liver dysfunction in sepsis. *Adv Clin Exp Med*. 2018;27(4):547-51. doi: [10.17219/acem/68363](https://doi.org/10.17219/acem/68363)
- Zhao J, He Y, Xu P, Liu J, Ye S, Cao Y. Serum ammonia levels on admission for predicting sepsis patient mortality at D28 in the emergency department: A 2-center retrospective study. *Medicine (Baltimore)*. 2020;99(11):e19477. doi: [10.1097/MD.00000000000019477](https://doi.org/10.1097/MD.00000000000019477)
- Numan Y, Jawaid Y, Hirzallah H, Kusmic D, Megri M, Aqtash O, et al. Ammonia vs. Lactic Acid in Predicting Positivity of Microbial Culture in Sepsis: The ALPS Pilot Study. *J Clin Med*. 2018;7(8):182. doi: [10.3390/jcm7080182](https://doi.org/10.3390/jcm7080182)
- Shulyatnikova TV, Tumanskiy VO. Immunohistochemical expression of GFAP, GS, AQP4, Alzheimer-2-astrocytosis and brain ammonia levels in deceased septic patients without liver failure and those with sepsis-associated liver injury. *Art of Medicine*. 2023;2(26):138-45. doi: [10.21802/artm.2023.2.26.138](https://doi.org/10.21802/artm.2023.2.26.138)
- Gutiérrez-de-Juan V, López de Davalillo S, Fernández-Ramos D, Barberer-Torres L, Zubiete-Franco I, Fernández-Tussy P, et al. A morphological method for ammonia detection in liver. *PLoS One*. 2017;12(3):e0173914. doi: [10.1371/journal.pone.0173914](https://doi.org/10.1371/journal.pone.0173914)
- Long MT, Coursin DB. Undifferentiated non-hepatic hyperammonemia in the ICU: Diagnosis and management. *J Crit Care*. 2022;70:154042. doi: [10.1016/j.jcrc.2022.154042](https://doi.org/10.1016/j.jcrc.2022.154042)
- Sakusic A, Sabov M, McCambridge AJ, Rabinstein AA, Singh TD, Mukesh K, et al. Features of Adult Hyperammonemia Not Due to Liver Failure in the ICU. *Crit Care Med*. 2018;46(9):e897-e903. doi: [10.1097/CCM.0000000000003278](https://doi.org/10.1097/CCM.0000000000003278)
- Jaeger V, DeMorrow S, McMillin M. The Direct Contribution of Astrocytes and Microglia to the Pathogenesis of Hepatic Encephalopathy. *J Clin Transl Hepatol*. 2019;7(4):352-61. doi: [10.14218/JCTH.2019.00025](https://doi.org/10.14218/JCTH.2019.00025)
- Agarwal AN, Mais DD. Sensitivity and Specificity of Alzheimer Type II Astrocytes in Hepatic Encephalopathy. *Arch Pathol Lab Med*. 2019;143(10):1256-8. doi: [10.5858/arpa.2018-0455-OA](https://doi.org/10.5858/arpa.2018-0455-OA)
- Akhoundzadeh K, Shafia S. Association between GFAP-positive astrocytes with clinically important parameters including neurological deficits and/or infarct volume in stroke-induced animals. *Brain Res*. 2021;1769:147566. doi: [10.1016/j.brainres.2021.147566](https://doi.org/10.1016/j.brainres.2021.147566)
- Heming N, Mazeraud A, Verdonk F, Bozza FA, Chrétien F, Sharshar T. Neuroanatomy of sepsis-associated encephalopathy. *Crit Care*. 2017;21(1):65. doi: [10.1186/s13054-017-1643-z](https://doi.org/10.1186/s13054-017-1643-z)
- Elsherbini DM, Ghoneim FM, El-Mancy EM, Ebrahim HA, El-Sherbiny M, El-Shafey M, et al. Astrocytes profiling in acute hepatic encephalopathy: Possible enrolling of glial fibrillary acidic protein, tumor necrosis factor-alpha, inwardly rectifying potassium channel (Kir 4.1) and aquaporin-4 in rat cerebral cortex. *Front Cell Neurosci*. 2022;16:896172. doi: [10.3389/fncel.2022.896172](https://doi.org/10.3389/fncel.2022.896172)
- Sepehrinezhad A, Zarifkar A, Namvar G, Shahbazi A, Williams R. Astrocyte swelling in hepatic encephalopathy: molecular perspective of cytotoxic edema. *Metab Brain Dis*. 2020;35(4):559-78. doi: [10.1007/s11011-020-00549-8](https://doi.org/10.1007/s11011-020-00549-8)
- Filchenko I, Blochet C, Buscemi L, Price M, Badaut J, Hirt L. Caveolin-1 Regulates Perivascular Aquaporin-4 Expression After Cerebral Ischemia. *Front Cell Dev Biol*. 2020;8:371. doi: [10.3389/fcell.2020.00371](https://doi.org/10.3389/fcell.2020.00371)
- Riba M, Augé E, Campo-Sabariz J, Moral-Anter D, Molina-Porcel L, Ximelis T, et al. Corpora amylacea act as containers that remove waste products from the brain. *Proc Natl Acad Sci U S A*. 2019;116(51):26038-48. doi: [10.1073/pnas.1913741116](https://doi.org/10.1073/pnas.1913741116)
- Zemtsova I, Görg B, Keitel V, Bidmon HJ, Schrör K, Häussinger D. Microglia activation in hepatic encephalopathy in rats and humans. *Hepatology*. 2011;54(1):204-15. doi: [10.1002/hep.24326](https://doi.org/10.1002/hep.24326)